

Catalytic C₃H₆ Oxidation Triggered by Plasma

Y. -H. Song, W. S. Kang, D. H. Lee, and J. O. Lee

Korea Institute of Machinery & Materials, Korea

Abstract—Oxidation of C₃H₆ at low temperature has been investigated using a combined plasma-catalyst process. The plasma-catalyst reactor consisted of a honeycomb-structured monolith substrate, which was the same as the one adopted in the automobile industry, and a couple of wire-mesh metal electrodes. When high-voltage AC power was applied to the plasma-catalyst reactor, a stable plasma was generated in the gap between the electrode and the substrate. The geometrical configuration of the present plasma-catalyst reactor was categorized as a post-plasma catalyst reactor in which gases are oxidized in two separate processes; plasma oxidation occurs first, following which the emitted gases from the plasma reactor are treated in the catalyst reactor. Tests for C₃H₆ oxidation were conducted for temperatures that ranged from room temperature to 200°C. When the operating temperature was lower than the light-off temperature of the catalyst, total hydrocarbon (THC) concentration dropped abruptly immediately following the plasma triggering. This reduced THC quickly recovered as soon as the plasma process was terminated. On the other hand, when the temperature was higher than the light-off temperature, the temporal variations of THC were relatively slower due to adsorption and desorption processes. Additional tests showed that the desorption process triggered by plasma competed with the oxidation process, which could even result in an increase of THC emission under certain operating conditions.

Keywords—Non-thermal plasma, honeycomb-structured catalyst, temporal evolution

I. INTRODUCTION

Combining plasma and catalyst processes for low-temperature oxidation of diluted VOCs or hydrocarbons is a very promising technology [1-5]. Compared to the exclusively plasma based process, the combined process offers better performances, such as higher DRE (Destruction Rate Efficiency), fewer by-product generation, and lower power consumption. These advantages of the combined process are attributed to the outcomes of various plasma-catalyst interactions, such as enhanced electrical field and extended spatial distribution of discharge in the presence of catalytic substrates [1-3, 6-8], generation of micro discharge and short-living chemically active species in the catalytic pores [9-10], changes of surface chemistry by discharge [11-13], and improved surface area and structure [14-16]. The synergetic effects of the combined process are observed as well, even though the plasma zone is spatially separated from the catalyst. In this case, the long-living species, e.g. O₃, generated in the plasma zone and the increased retention time of the treated gases or the oxygen contribute to the enhanced performance of the combined process [4-5, 17-23].

One of the issues with the combined plasma-catalyst process is finding an appropriate reactor geometry that can accommodate high gas flow rate [21-26]. So far, packed-bed type plasma reactors, in which catalyst beads are packed into the reactor, have been extensively investigated. However, in the packed-bed type reactors the pressure at a high gas flow rate becomes too high. Thereby, from the practical point of view, a technique of plasma generation utilizing a honeycomb-structured

catalyst, producing low pressure loss and widely adopted in the industry, is worth investigating. In this regard, a simple and compact plasma-catalyst reactor, in which a honeycomb-structured catalyst was adopted, was proposed in the present study. The plasma generation mechanism and the characteristics of the proposed plasma reactor will be discussed below.

A small-scale C₃H₆ oxidation experiment utilizing the proposed plasma-catalyst reactor has been conducted to investigate the technical potential for automobile applications. Due to the tightening regulations on CO₂ emission from automobile, various innovative technologies of engine and exhaust treatment have been proposed recently [24-31]. Interestingly, even the EHC (Electrically Heated Catalyst) technology for cold-start engine, which has not been adopted for a couple of decades due to excessive consumption of electrical power, has been intensively investigated recently [30, 31], because an electrically controlled catalyst technology, including the plasma-catalyst technology, is ideal for the current automobile concepts featuring energy recuperation and start-stop functioning. Motivated by this, a study of C₃H₆ oxidation at low temperature was conducted as an early stage of the study of plasma-catalyst technology for vehicle applications. The tested temperatures of the plasma-catalyst oxidation process ranged from room temperature to 200°C. The emissions from the plasma-catalyst reactor were detected at the rate of one sample per second, which provided information about the temporal evolution of C₃H₆ oxidation.

II. METHODOLOGY

A. Plasma Generation

Fig. 1 shows a schematic diagram of the proposed plasma generation technique. The plasma generator

Corresponding author: Young-Hoon Song
e-mail address: yhsong@kimm.re.kr

Presented at the 9th International Symposium on Non-Thermal/Thermal Plasma Pollution Control Technology & Sustainable Energy, in June 2014

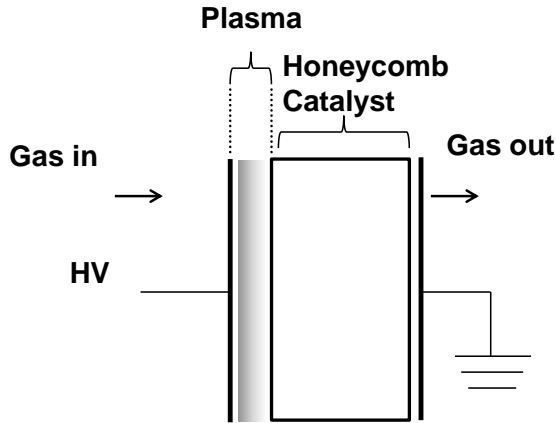


Fig. 1. Schematic diagram of plasma generator with honeycomb-structured monolith substrate.

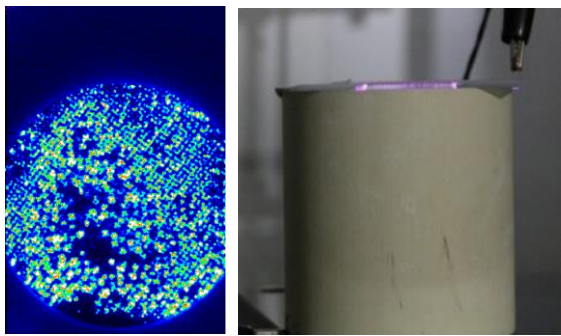


Fig. 2. Front and side views of the catalyst during the micro-discharge generation (intensified CCD camera (Princeton Instruments) was used for the front view).

consists of a honeycomb-structured monolith substrate and a couple of metal wire-mesh electrodes. The monolith substrate is a commercialized automobile part, and consists of 400 cells per square inch. As shown in Fig. 1, high voltage was applied to the substrate and the electrodes. The peak voltage typically ranged from 8 kV to 20 kV. The AC power frequency varied from 60 Hz to 2 kHz. Under such wide range of operating conditions, stable plasma was generated in the gap between the catalyst substrate and the electrode, as shown in Fig. 2.

Preliminary tests showed that the characteristics of plasma generation with the honeycomb-structured substrate are affected by several catalyst properties, such as the coating materials (Al_2O_3 , Pt- Al_2O_3 , and zeolite), substrate's length, and temperature. In the present study, the substrate was coated with Pt- Al_2O_3 (platinum loading: 0.507%), and cut into a small piece (20 mm thick and 40 mm long) to place the catalyst into the electrical oven. Fig. 3 shows the voltage and current oscillograms. Here, the current and voltage were detected by voltage and current probes equipped with a digital oscilloscope (P6015A and TCP0030 with DPO5054, Tektronix, Inc.). As shown in Fig. 3, the discharge current peaks were detected during the positive rising phase of the applied voltage. This current pattern looks like a typical current pattern of DBD (Dielectric Barrier Discharge), although the current pattern during the negative phase is not shown. The current pattern in Fig. 3

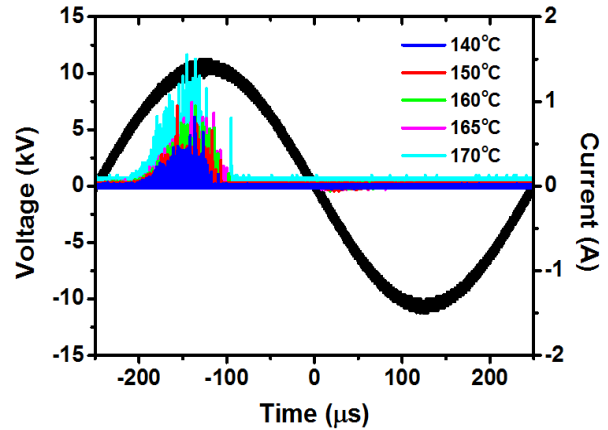


Fig. 3. Voltage and current oscillograms, Operating temperatures: 140-160°C, peak voltage: 12 kV, frequency: 2 kHz.

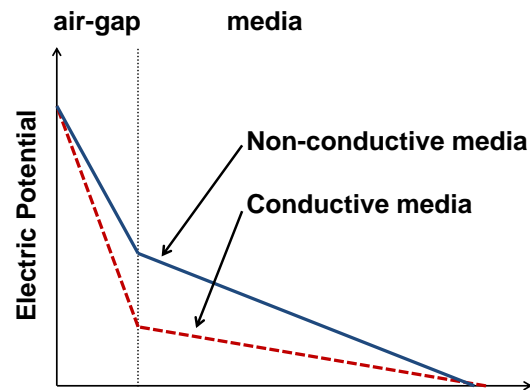


Fig. 4. Schematic diagram of electrical potential across the catalyst and the gap.

indicated that the catalyst made of the ceramics serves as a dielectric barrier that inhibits transition into a spark and distributes the micro-discharge all over the surface.

The authors believe that the present catalyst plays two roles in a high electrical field; it serves as a dielectric barrier and as a conductive medium [26]. Results of several tests showed that the conductive nature of the catalyst is noticeable, especially at high temperatures. For instance, as shown in Fig. 3, the current peaks increased at higher ambient temperature. This phenomenon should be related to the increased electrical conductance of the catalyst, and can be explained as follows by using the schematic in Fig. 4. The catalyst's conductance at high temperature is assumed to be higher, which decreases the electrical potential across the catalyst. As shown in Fig. 4, the decreased electrical potential of the catalyst results in the increased potential difference between the narrow gap. Because of the increased potential difference, the current peaks at higher temperatures were higher than those at lower temperatures. Thus, we hypothesized that the catalyst has conductive properties.

Additional evidence for the conductive nature of the catalyst is provided by the Lissajous charge-voltage plot. As shown in Fig. 5, the Lissajous plot at 160°C has elliptical shape, and differs from a sharp parallelogram

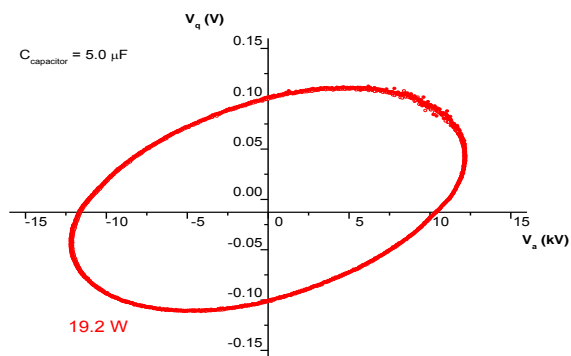
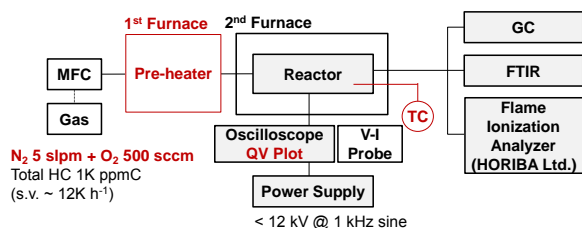


Fig. 5. Elliptical Lissajous plot at 160°C.

Fig. 6. Experimental apparatus for C_3H_6 oxidation.

observed in a typical DBD. This elliptical shape was obtained only at high temperatures, and returned to a parallelogram at low temperatures. A similar result, i.e. an elliptical shape of Lissajous plot of a plasma-catalyst reactor at high temperature, was also reported by Harling *et al.* [32]. As Kogelshatz stated [33], the resistive load in the DBD generator results in such elliptical Lissajous plot. The two observations, stronger current peaks and elliptical Lissajous plot at high temperature, supported the notion that the present catalyst serves as a dielectric barrier and a conductive medium.

B. Experimental Apparatus for C_3H_6 Oxidation

Fig. 6 is a schematic diagram of the test apparatus for the C_3H_6 oxidation experiment. A gas mixture containing 900 parts per million carbon (ppmC) of C_3H_6 , 5 standard liters per minute (lpm) of nitrogen, and 500 standard cubic centimeters per minute (ccm) of oxygen was supplied to the pre-heater and the reactor. In the C_3H_6 oxidation test, the honeycomb monolith catalyst (catalyst thickness of 20 mm and diameter of 40 mm) was used. With this catalyst's volume and gas flow rate, the space velocity of the catalyst was estimated to be $1,200\text{ h}^{-1}$. The temperature was controlled in the second furnace, and was detected at the outlet section of the reactor. Typically, the power supply was operated with the voltage of 8-12 kV at the frequency of 2 kHz. The discharge power, estimated using the Lissajous plot, ranged from 2.4 W to 5.7 W. Thereby, the specific energy density [J/L] in the present study ranged from 26 J/L to 62 J/L. The THC concentrations at the outlet were measured at the rate of one sample per second in ppmC using a flame ionization analyzer (MEXA-1170HFID, Horiba, Ltd.).

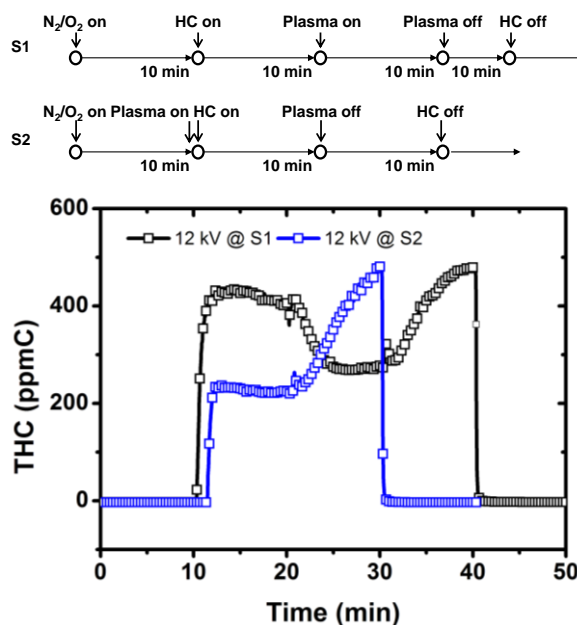


Fig. 7. Temporal evolution of THC emission in different operating scenarios. Scenario 1: plasma process starts 10 minutes following the C_3H_6 injection, Scenario 2: both "plasma on" and C_3H_6 injection start at the same time. Initial operating temperature: 160°C, Input THC concentration: 900 ppmC, Applied voltage: 12 kV.

III. RESULTS AND DISCUSSION

Fig. 7 shows the temporal evolution of THC concentrations detected at the outlet of the plasma-catalyst reactor using the flame ionization detector. The tests were conducted in accordance with two different test procedures. In the first procedure, the plasma process started 10 minutes following the C_3H_6 injection into the reactor (scenario 1). In the second procedure, the plasma process and the C_3H_6 injection were simultaneously initiated (scenario 2). The initial operating temperature in these tests was set to 160°C. On the other hand, as shown in Fig. 8, the light-off temperature of the catalyst, corresponding to the temperature at which the conversion rate was 50%, was about 158°C. In scenario 1, 400 ppmC of the THC were maintained for 10 minutes following the C_3H_6 injection. The initial decrease of THC from 900 ppmC to 400 ppmC was attributed to the thermally activated catalyst. Ten minutes later, when the plasma process started, the THC concentration decreased gradually for 5 minutes, and reached a steady-state. In scenario 2, 220 ppmC of THC was detected at the beginning of the plasma process, and remained the same throughout the plasma process. In both cases, THC concentration increased gradually after the plasma process was terminated.

The above oxidation test showed that plasma-catalyst process at high temperature is not an instantaneous process that is observed in exclusively plasma-based process. Such gradual THC variation was attributed to the adsorption-desorption behavior of the hydrocarbons on the catalytic surface. Also, the test showed that the final THC concentration of the plasma-catalyst process is

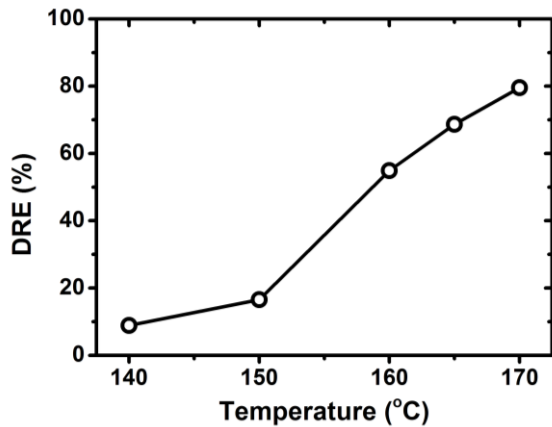


Fig. 8. DRE (Destruction Rate Efficiency) of the catalyst as a function of operating temperature.

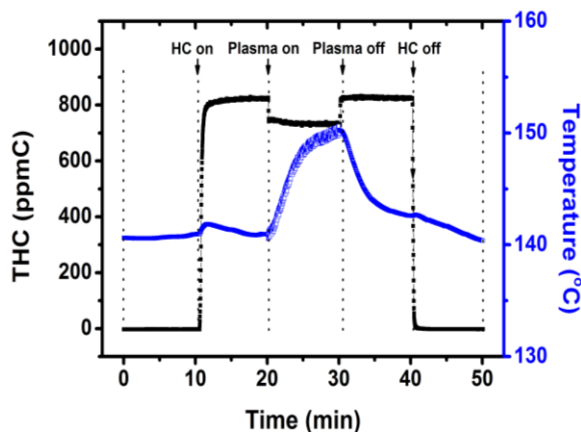


Fig. 9. Temporal evolution of THC. Starting temperature: 140°C, Applied voltage: 12 kV.

different, depending on the operating scenario of the plasma-catalyst process. In scenario 1, because the hydrocarbons are already adsorbed on the catalytic surface before the plasma process, the pre-adsorbed hydrocarbons could result in such relatively low conversion rate of hydrocarbons.

Consecutive tests showed that the adverse effects of pre-adsorbed hydrocarbons to the plasma-catalytic process were significant, especially when the initial temperature was higher than the light-off temperature. As shown in Figs. 9 and 10, the characteristics of the THC's temporal evolution differed depending on the operating temperatures; in one case the temperature was lower than the light-off temperature and in another case it was higher than the light-off-temperature. In these tests, the plasma process started 10 minutes following the C_3H_6 injection, as in scenario 1. When the initial temperature was 140°C, which was lower than the light-off temperature, the temporal evolution of the THC was straightforward. Immediately following the plasma process initiation, the THC dropped abruptly. This reduced THC quickly recovered after the plasma process was terminated. The DRE of the plasma-catalyst process immediately following the plasma process initiation was

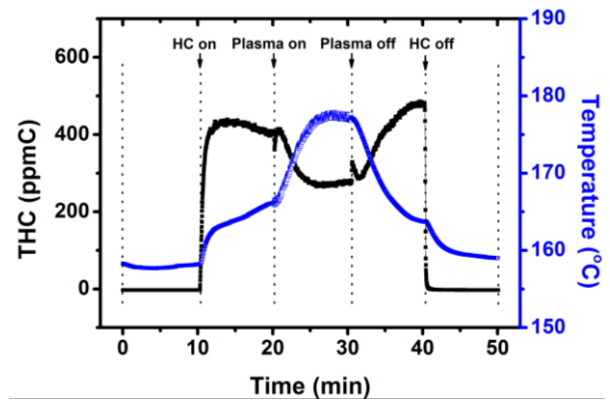


Fig. 10. Temporal evolution of THC, starting temp. 155°C, applied voltage: 12 kV.

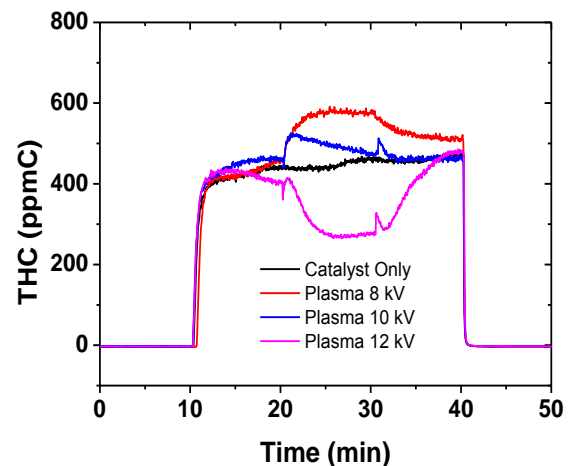


Fig. 11. Temporal evolution of THC at different voltages. 8 kV: 2.4 W, 10 kV: 3.8 W, 12 kV: 5.3 W, Temp.: 160°C.

about 20%, which as expected was higher than that of the catalyst only process at 140°C.

When the starting temperature was 155°C, the THC evolution was more complicated compared with the previous case. As shown in Fig. 10, the THC variations triggered by "plasma on" (420 ppmC \rightarrow 280 ppmC) and "plasma off" (280 ppmC \rightarrow 500 ppmC) proceeded gradually. While the THC concentration was gradually decreasing, the temperature was also slowly increasing, eventually reached 178°C. At 178°C, the DRE of the plasma-catalyst process was about 70%. Interestingly, this DRE was apparently lower than that of the catalyst only process at 170°C, i.e. 80% (see Fig. 8, DRE of the catalyst only process). In addition, the final THC concentration (500 ppmC) are higher than the initial one (420 ppmC). Again, the gradual decrease of the THC concentration and the relatively low conversion rates of the plasma-catalyst process were observed at higher temperatures. As mentioned earlier, the pre-adsorbed hydrocarbons could result in such poor plasma-catalytic process.

Further investigation regarding the effects of the adsorption on the process was conducted by changing the applied voltage. Fig. 11 shows three different THC evolution plots at 160°C. At 8 kV, the THC

concentration increased rapidly during the earlier stage and eventually reached a stable state. At 10 kV, desorption was again observed during the earlier stage and diminished gradually during the later stage. At 12 kV, THC emissions dropped by supplying the electrical power.

Fig. 11 clearly shows that there exists a critical condition for the THC reduction. In other cases, supplying the electrical power even increased the THC emission from the reactor. The critical condition was not anticipated before the test. Whether or not this critical condition was anticipated, result of this test indicated that oxidation process competed with the desorption process, and predominated at a certain power. Conversely, this finding could imply that desorption process could be started with a little power, compared to the power required for the oxidation to start. At present, detailed understanding of desorption process in the present reactor is not available, since desorption could be driven by several mechanisms, such as heated catalytic surface by dielectric heating and resistive heating, plasma-driven desorption [20], and electrically modified desorption-adsorption equilibrium [34]. Further research is needed to clarify the plasma-triggered desorption mechanism.

Similar to desorption, the oxidation in the present reactor at high temperature was also driven by the simultaneous thermal activation of the catalyst and plasma. As shown in Figs. 10 and 11, abrupt THC variations were observed immediately following "plasma on" and "plasma off" events. This implies that plasma-driven oxidation, which is a fast reaction process and is not relevant to the temperature condition, somehow contributes to the oxidation process in the plasma-catalyst reactor. Similar to desorption, further investigation is needed to decouple the contributions of the plasma-driven reactions from those of the thermally driven catalytic reactions.

The geometry of the present plasma-catalyst reactor can be categorized as a post-plasma catalysis reactor that consists of two separated reaction zones; the plasma zone and the catalyst zone. As pointed out by Roland *et al.* [35] and Kirkpatrick *et al.* [28], in the case of a post-plasma catalysis reactor, the long-living species generated in the plasma zone, i.e. O₃, plays a major role, and can deactivate the catalyst. Although the present plasma-catalyst process was conducted using the post-plasma catalysis reactor, the effects of the above mentioned deactivation were not clearly observed. After the THC concentrations reached a steady state, as shown in Figs. 9 and 10, the THC concentrations remained constant for 5-10 minutes. In the present tests, after each oxidation test, the catalyst was regenerated with air under the high temperature conditions (200°C).

IV. CONCLUSION

One of the objectives of the present study was to evaluate the feasibility of the proposed plasma-catalyst reactor, in which a honeycomb-structured catalyst

adopted in automobile exhaust system is used. The test showed that stable plasma can be generated in the narrow gap between the wire-mesh metal electrode and the catalyst. Here, the catalyst made of cordierite materials served as a dielectric barrier. Additional tests in various temperature conditions showed that the catalyst had a conductive properties, too, which resulted in stronger current peaks and elliptic Lissajous plot at high temperatures.

Several important characteristics of the present plasma-catalyst process were discussed, such as the adverse effects of adsorption on the C₃H₆ oxidation, and temperature condition required for the adsorption-desorption processes, etc. The tests clearly showed that the adsorbed hydrocarbons hinder oxidation process, which results in lower conversion rate and slows the oxidation process. Further investigations revealed that the reason for such adverse effects could be attributed to the competition between the oxidation and desorption processes.

ACKNOWLEDGMENT

This work was financially supported by the Korea Research Council for Industrial Science and Technology (ISTK).

REFERENCES

- [1] H. H. Kim and A. Ogata, "Nonthermal plasma activates catalyst: from current understanding and future prospects," *European Physical Journal-Applied Physics*, vol. 55, 2011.
- [2] J. Van Durme, J. Dewulf, C. Leys, and H. Van Langenhove, "Combining non-thermal plasma with heterogeneous catalysis in waste gas treatment: A review," *Applied Catalysis B-Environmental*, vol. 78, pp. 324-333, 2008.
- [3] K. Urashima and J. S. Chang, "Removal of volatile organic compounds from air streams and industrial flue gases by non-thermal plasma technology," *IEEE Transactions on Dielectrics and Electrical Insulation*, vol. 7, pp. 602-614, 2000.
- [4] H. L. Chen, H. M. Lee, S. H. Chen, M. B. Chang, S. J. Yu, and S. N. Li, "Removal of Volatile Organic Compounds by Single-Stage and Two-Stage Plasma Catalysis Systems: A Review of the Performance Enhancement Mechanisms, Current Status, and Suitable Applications," *Environmental Science & Technology*, vol. 43, pp. 2216-2227, 2009.
- [5] A. M. Vandembroucke, R. Morent, N. De Geyter, and C. Leys, "Non-thermal plasmas for non-catalytic and catalytic VOC abatement," *Journal of Hazardous Materials*, vol. 195, pp. 30-54, 2011.
- [6] W. S. Kang, J. M. Park, Y. Kim, and S. H. Hong, "Numerical study on influences of barrier arrangements on dielectric barrier discharge characteristics," *IEEE Transactions on Plasma Science*, vol. 31, pp. 504-510, 2003.
- [7] S. Jo, D. H. Lee, W. S. Kang, and Y. H. Song, "Effect of packing material on methane activation in a dielectric barrier discharge reactor," *Physics of Plasmas*, vol. 20, 2013.
- [8] H. J. Gallon, X. Tu, and J. C. Whitehead, "Effects of Reactor Packing Materials on H₂ Production by CO₂ Reforming of CH₄ in a Dielectric Barrier Discharge," *Plasma Processes and Polymers*, vol. 9, pp. 90-97, 2012.
- [9] U. Roland, F. Holzer, and F. D. Kopinke, "Improved oxidation of air pollutants in a non-thermal plasma," *Catalysis Today*, vol. 73, pp. 315-323, 2002.
- [10] F. Holzer, U. Roland, and F. D. Kopinke, "Combination of non-thermal plasma and heterogeneous catalysis for oxidation of

- volatile organic compounds Part 1. Accessibility of the intra-particle volume," *Applied Catalysis B-Environmental*, vol. 38, pp. 163-181, 2002.
- [11] H. H. Kim, A. Ogata, M. Schiorlin, E. Marotta, and C. Paradisi, "Oxygen Isotope ($^{18}\text{O}_2$) Evidence on the Role of Oxygen in the Plasma-Driven Catalysis of VOC Oxidation," *Catalysis Letters*, vol. 141, pp. 277-282, 2011.
- [12] H. H. Kim, A. Ogata, and S. Futamura, "Oxygen partial pressure-dependent behavior of various catalysts for the total oxidation of VOCs using cycled system of adsorption and oxygen plasma," *Applied Catalysis B-Environmental*, vol. 79, pp. 356-367, 2008.
- [13] Y. F. Guo, D. Q. Ye, K. F. Chen, J. C. He, and W. L. Chen, "Toluene decomposition using a wire-plate dielectric barrier discharge reactor with manganese oxide catalyst in situ," *Journal of Molecular Catalysis a-Chemical*, vol. 245, pp. 93-100, 2006.
- [14] C. J. Liu, K. L. Yu, Y. P. Zhang, X. L. Zhu, F. He, and B. Eliasson, "Characterization of plasma treated Pd/HZSM-5 catalyst for methane combustion," *Applied Catalysis B-Environmental*, vol. 47, pp. 95-100, 2004.
- [15] C. J. Liu, J. J. Zou, K. L. Yu, D. G. Cheng, Y. Han, J. Zhan, C. Ratanatawanate, and B. W. L. Jang, "Plasma application for more environmentally friendly catalyst preparation," *Pure and Applied Chemistry*, vol. 78, pp. 1227-1238, 2006.
- [16] M. Sugawara and A. Ogata, "Effect of Different Combinations of Metal and Zeolite on Ozone-Assisted Catalysis for Toluene Removal," *Ozone: Science & Engineering*, vol. 33, pp. 158-163, 2011.
- [17] A. M. Harling, D. J. Glover, J. C. Whitehead, and K. Zhang, "The role of ozone in the plasma-catalytic destruction of environmental pollutants," *Applied Catalysis B-Environmental*, vol. 90, pp. 157-161, 2009.
- [18] A. Naydenov, P. Konova, P. Nikolov, F. Klingstedt, N. Kumar, D. Kovacheva, P. Stefanov, R. Stoyanova, and D. Mehandjiev, "Decomposition of ozone on Ag/SiO₂ catalyst for abatement of waste gases emissions," *Catalysis Today*, vol. 137, pp. 471-474, 2008.
- [19] M. Magureanu, N. B. Mandache, P. Eloy, E. M. Gaigneaux, and V. I. Parvulescu, "Plasma-assisted catalysis for volatile organic compounds abatement," *Applied Catalysis B-Environmental*, vol. 61, pp. 12-20, 2005.
- [20] Y. H. Song, S. J. Kim, K. I. Choi, and T. Yamamoto, "Effects of adsorption and temperature on a nonthermal plasma process for removing VOCs," *Journal of Electrostatics*, vol. 55, pp. 189-201, 2002.
- [21] K. Hensel, S. Katsura, and A. Mizuno, "DC microdischarges inside porous ceramics," *IEEE Transactions on Plasma Science*, vol. 33, pp. 574-575, 2005.
- [22] S. Sato, K. Hensel, H. Hayashi, K. Takashima, and A. Mizuno, "Honeycomb discharge for diesel exhaust cleaning," *Journal of Electrostatics*, vol. 67, pp. 77-83, 2009.
- [23] T. Kuroki, T. Fujioka, M. Okubo, and T. Yamamoto, "Toluene concentration using honeycomb nonthermal plasma desorption," *Thin Solid Films*, vol. 515, pp. 4272-4277, 2007.
- [24] T. Hammer, "Non-thermal plasma application to the abatement of noxious emissions in automotive exhaust gases," *Plasma Sources Science & Technology*, vol. 11, pp. A196-A201, 2002.
- [25] M. J. Kirkpatrick, E. Odic, S. Zinola, and J. Lavy, "Plasma assisted heterogeneous catalytic oxidation: HCCI Diesel engine investigations," *Applied Catalysis B-Environmental*, vol. 117, pp. 1-9, 2012.
- [26] W. S. Kang, D. H. Lee, J. O. Lee, M. Hur, and Y. H. Song, "Combination of Plasma with a Honeycomb-Structured Catalyst for Automobile Exhaust Treatment," *Environmental Science & Technology*, vol. 47, pp. 11358-11362, 2013.
- [27] D. H. Lee, K. T. Kim, M. S. Cha, J. O. Lee, Y. H. Song, H. Cho, Y. S. Kim, Y. Song, and T. Jee, "Active Regenerative DPF Using a Plasma Assisted Burner," *SAE Technical Paper*, 2009-01-1926, 2009.
- [28] M. J. Kirkpatrick, E. Odic, J. P. Leininger, G. Blanchard, S. Rousseau, and X. Glipa, "Plasma assisted heterogeneous catalytic oxidation of carbon monoxide and unburned hydrocarbons: Laboratory-scale investigations," *Applied Catalysis B-Environmental*, vol. 106, pp. 160-166, 2011.
- [29] A. S. zu Schweinsberg, M. Klenk, and A. Degen, "Engine-independent exhaust gas aftertreatment using a burner heated catalyst," *SAE Technical Paper*, 2006-01-3401, 2006.
- [30] C. H. Kim, M. Paratore, E. Gonze, C. Solbrig, and S. Smith, "Electrically heated catalysts for cold-start emissions in diesel aftertreatment," *SAE Technical Paper*, 2012-01-1092, 2012.
- [31] M. Presti and L. Pace, "An alternative way to reduce fuel consumption during cold start: the electrically heated catalyst," *SAE Technical Paper*, 2011-24-0178, 2011.
- [32] A. M. Harling, H. H. Kim, S. Futamura, and J. C. Whitehead, "Temperature dependence of plasma-catalysis using a nonthermal, atmospheric pressure packed bed; the destruction of benzene and toluene," *Journal of Physical Chemistry C*, vol. 111, pp. 5090-5095, 2007.
- [33] U. Kogelschatz, "Dielectric-barrier discharges: Their history, discharge physics, and industrial applications," *Plasma Chemistry and Plasma Processing*, vol. 23, pp. 1-46, 2003.
- [34] N. Blin-Simiand, P. Tardiveau, A. Risacher, F. Jorand, and S. Pasquiers, "Removal of 2-heptanone by dielectric barrier discharges - The effect of a catalyst support," *Plasma Processes and Polymers*, vol. 2, pp. 256-262, 2005.
- [35] U. Roland, F. Holzer, and E. D. Kopinke, "Combination of non-thermal plasma and heterogeneous catalysis for oxidation of volatile organic compounds Part 2. Ozone decomposition and deactivation of $\gamma\text{-Al}_2\text{O}_3$," *Applied Catalysis B-Environmental*, vol. 58, pp. 217-226, 2005.